Studies on three-way catalysis with supported gold catalysts. Influence of support and water content in feed

Viktor Ulrich [a], Boris Moroz [b,c], Ilya Sinev [a], Pavel Pyriaev [b], Valerii Bukhtiyarov [b,c], Wolfgang Grünert [a,*]

[a] Lehrstuhl für Technische Chemie, Ruhr-Universität Bochum, D-44780 Bochum, Germany
[b] Boreskov Institute of Catalysis, Novosibirsk 630090, Russian Federation
[c] Novosibirsk State University, Novosibirsk 630090, Russian Federation

ABSTRACT

The potential of gold for the reactions of three-way catalysis was examined by converting a model exhaust consisting of 1.1% CO, 0.1% propene, 0.1% NO, O_2 (0.95% - stoichiometric, 0.85% - rich, or 1.05% - lean), and water (10% or none) over catalysts containing 1–2 wt-% Au supported on Al_2O_3, La-Al_2O_3, TiO_2, and $CeZrO_x$ supports. For comparison, CO and propene were also reacted stoichiometrically with oxygen in absence of further reactants, likewise, reduction of NO with CO was examined. It was found that propene is a strong poison for CO oxidation, but the intensity of the poisoning effect depended on the support (Al_2O_3 > La-Al_2O_3 > TiO_2 > $CeZrO_x$). The poisoning was strongest in dry feed but was partly alleviated in moist feed. NO was poorly converted both in the TWC mixture and in binary feed. In the model exhaust, NO conversion resulted in significant N_2O formation at low temperatures, but selectivity to N_2 increased with temperature. Despite poisoning by propene, Au/$CeZrO_x$ outperformed a commercial reference catalyst in CO and propene oxidation. Calcination in moist dilute air at 923 K inflicted only moderate damage to the Au catalysts. Over Au/$CeZrO_x$, CO oxidation in stoichiometric feed was not significantly affected at all, but the poisoning effect of propene became more severe in the TWC model feed. Analogous treatment at 1223 K resulted in inacceptable damage to all reactions involved and on all supports.

© 2016 Elsevier B.V. All rights reserved.

1. Introduction

Research on gold catalysts has attracted huge attention during the past three decades. Among gas-phase redox reactions catalyzed by supported Au nanoparticles are CO oxidation in the absence or presence of H_2 [1–3], the oxidation of volatile organic compounds [4], water gas shift [5], alkane oxidation [6,7], propene epoxidation [8], the synthesis of hydrogen peroxide [9], and hydrochlorination of acetylene [10] (see also reviews in [11]). While attention has meanwhile shifted to liquid-phase reactions, e.g. the selective oxidation of alcohols, glycerol [12,13] and of other oxygenated molecules [11], it turns out that three-way catalysis (TWC) has hardly ever been a topic in the open literature on gold catalysis. This is surprising because the high oxidation activity of gold might allow for solving cold-start problems while literature data on gold activity in the reduction of NO by CO and by H_2 [14] and even in

the selective reduction of NO by propene in presence of O_2 [14–17] suggest that Au might be able to catalyze NO reduction also in the exhaust of gasoline cars.

To our best knowledge, there is only one study of TWC with gold-containing catalysts in the open literature. Mellor et al. [18] converted simulated effluent (net oxidizing or reducing) in stationary regime over a catalyst containing 1% Au on a mixed support comprising CeZrOx, ZrO_2, anatase, and various promoters. The results confirmed expectations as far as related to CO oxidation while hydrocarbon oxidation was more sluggish though proceeding still in the temperature range of interest. NO could be converted in the reducing feed over the monometallic catalyst with a light-off temperature T_{50} of 650 K, which was decreased by 80 K by addition of 0.1 wt-% Rh. Although no significant NO conversion was observed in net oxidizing feed, this result suggests that the full functionality of a three-way catalyst might be achieved even with a monometallic Au catalyst under fluctuating feed composition (λ oscillations) if the catalyst is endowed with appropriate storage properties.

The problem expected in the use of gold in TWC is rather related to catalyst stability because three-way catalysts are at least temporarily exposed to temperatures around the melting point of bulk

* Corresponding author at: Lehrstuhl für Technische Chemie, Ruhr-Universität Bochum, P. O. Box 102148, D-44780 Bochum, Germany.
E-mail address: w.gruenert@techem.ruhr-uni-bochum.de (W. Grünert).

gold. Although appropriate preparations may result in surprising stabilization effects exerted by the support on supported Au nanoparticles [19–23], binding the gold in alloys may be a more promising route for the utilization of its potential in three-way catalysis. Our group has embarked on an exploration of the opportunities of such approach. In an first step, the catalytic behavior of gold alone on some typical supports (but without the additives used in Ref. [18]) has been studied, and first results related to the influence of the support and of moisture on activity, selectivity, and stability will be reported in the present communication.

2. Experimental

2.1. Catalysts

Gold nanoparticles were deposited on various supports: on Al_2O_3, on a La-stabilized Al_2O_3, on a mixed CeZrOx and on TiO_2. The Al_2O_3 used was PURALOX SCFa-140, which was donated by Sasol Germany GmbH, the La-stabilized alumina was obtained from the same source and contained ca. 2 wt-% La. The ceria-zirconia mixed oxide was a commercial product donated by Umicore & Co. KG Hanau (Germany) and was used without further analysis. The 1 wt-% Au/TiO_2 catalyst employed was AUROlite™ (Strem 79-0165 [24]). The reference TWC is a commercial sample donated by Interkat Katalysatoren GmbH (Königswinter, Germany), with a total precious metal content of ca. 2 wt.% consisting predominantly of Pd (Pd: Pt: Rh 13:1:1). The catalysts were compacted, crushed and sieved to get a 255–350 µm sieve fraction for the catalytic experiments.

Deposition of Au nanoparticles on Al_2O_3, La-Al_2O_3, and CeZrO$_x$ was achieved by the deposition-precipitation technique [25] using a procedure similar to that described previously [26]: A weighed amount of support dried at 383 K for 8 h immediately before catalyst preparation was shaken with an aqueous solution containing 2.5 mg Au per L for 1 h at 343 K. The solution had been obtained by neutralization of $HAuCl_4$ with NaOH to pH 7. After the interaction of support and Au solution, the powder was washed several times with large portions of warm distilled water (200 mL H_2O/g sample), dried in vacuo at room temperature overnight and calcined in air at 573 K for 4 h. Preparations were done with pre-granulated supports obtained by tableting support powder under a pressure of 106 N (pellet diameter 20 mm) for 60 min, crushing and sieving to 200–500 µm particles.

For stability studies, the catalysts were subjected to calcinations in a flow of 5% O_2 and 10% H_2O in He for 6 h at 923 K and 1223 K.

2.2. Characterization

The gold content of the catalyst samples was determined by X – ray Fluorescence on an ARL instrument equipped with a Rh anode (X-ray tube voltage: 50 kV, tube current: 40 mA, exposure time: 10 s). Textural characteristics of the supports were obtained from nitrogen physisorption measurements at 77 K by using an ASAP 2400 (Micromeritics) instrument. Before adsorption, the samples were outgassed at 573 K to a residual pressure of ca. 10^{-3} Torr. Specific surface areas and total pore volumes in the 3.5–100 nm range were calculated from the isotherms in the range of $p/p_0 = 0.05$–0.2 using the standard BET equation, and at $p/p_0 = 0.98$, respectively, mean pore diameters were derived from standard BJH analysis.

Transmission electron microscopy (TEM) studies were performed by using a JEM-2010 (JEOL, Japan) electron microscope with a lattice resolution of 0.14 nm and a 200 kV accelerating voltage. The mean diameters of gold particles for each catalyst sample were determined by counting over 300 particles in TEM images taken with a medium magnification and calculated by assuming a simple model of metal nanospheres [27].

X-ray photoelectron spectroscopy (XPS) studies were carried out on a SPECS spectrometer equipped with a PHOIBOS-150-MCD-9 hemispherical analyzer and a FOCUS-500 X-ray monochromator (Al Kα emission = 1486.6 eV, 150 W). Spectra were recorded with a constant pass energy of 20 eV. A low voltage electron flood gun was used for charge compensation. Quantitative analysis was performed using areas of XPS peaks integrated over Shirley backgrounds and corrected for the relative sensitivity factors (RSFs) taken from Ref. [28].

2.3. Catalytic studies

Catalytic measurements were performed in a microflow reactor (V4A-stainless steel) at atmospheric pressure in the temperature range 323–673 K using a temperature ramp of 5 K/min. Model feeds simulating stoichiometric, rich, and lean conditions were employed and consisted of CO (1.1%), NO (0.1%), and propene (0.1%), combined with O_2 (stoichiometric: 0.95 %; rich: 0.85%; lean: 1.05 %), H_2O (10 % or none), and He (balance). Following recent studies in literature [29,30], propene was chosen to represent unburned exhaust hydrocarbons because of the mostly unsaturated character of the latter and the wide range of carbon numbers spanning from (predominant) C_2 to >C_8 [31]. The mixture was fed to the reactor through electronic mass-flow controllers at a gas-hourly space velocity (GHSV) of 60,000 h^{-1} (183 ml/min feed on 125 mg catalyst). Steam was dosed by help of a saturator kept at 319 K. Subsequent tube connections were heated to 393 K. Before product analysis, moisture was removed from the effluent stream by a cold trap cooled with an ice bath. Effluent products were analyzed by a combination of calibrated mass spectrometry (O_2, NO, propene) and non-dispersive IR photometry (CO, CO_2, N_2O). The influence of the N_2O fragmentation pattern and its contribution the m/e = 30 (NO) QMS signal was taken into account in the evaluation of NO concentrations. CO, propene, and NO conversions of were calculated according to Eq. (1) (example – CO, index 0–initial)

$$X_{CO} = (c_{CO,0} - c_{CO})/c_{CO,0} \qquad (1)$$

N_2O formation will be reported as ppm content in the effluent. To describe catalyst activity, light-off temperatures T_{50} (T of 50% reactant conversion) were recorded and compared.

To examine interactions between reactants, oxidation of CO and of propene and reduction of NO by CO were also studied individually in the same setup. Feeds employed contained 1.1% CO, 0.55% O_2, and 10% (or no) H_2O in He for CO oxidation, 0.1% propene, 0.45% O_2, and 10% (or no) H_2O in He for propene oxidation, and 0.4% of both NO and CO for NO reduction (only dry feed). The GHSV was 60,000 h^{-1} in all cases. These experiments were made with Au on La-Al_2O_3 and on CeZrO$_x$.

3. Results

3.1. Characterization

In Table 1, basic data of the catalysts employed in this study are summarized. The Au content was 1.5–1.8 wt-% except for the commercial Au/TiO_2 catalyst where an Au content of 1 wt-% is specified. Texture data of catalysts on the basis of Al_2O_3 and TiO_2 are as expected for these supports. The values are very close to those of the pure supports, which have not been included. Apparently, loading of gold by deposition-precipitation (at least in quantities <2 wt-%) has little effect on the texture of these supports.

In Fig. 1, representative TEM micrographs of our catalysts are presented. Average Au particle sizes and particle size distributions

Table 1
Metal loadings, average particle sizes (TEM), and BET surface areas of Au catalysts.

Catalyst	Au (wt.%)	Average particle diameter (nm)[a]			Surface area ($m^2 g^{-1}$)	Mean pore diameter (nm)	Total pore volume ($cm^3 g^{-1}$)
		$\langle d_l \pm \sigma \rangle$	$\langle d_{vs} \rangle$	$\langle d_m \rangle$			
Au/Al_2O_3	1.8	1.5 ± 0.3	1.6	1.7	150	11.7	0.44
$Au/La-Al_2O_3$	1.8	1.7 ± 0.3	1.8	1.8	135	13.3	0.45
Au/TiO_2[b]	1	2–3	–	–	40–50	–	–
$Au/CeZrO_x$	1.55	2.8 ± 0.6	3.1	3.2	65	14.8	0.24

[a] $d_l = \sum d_i / \sum N$, $d_{vs} = \sum d_i^3 / \sum d_i^2$ and $d_m = \sum d_i^4 / \sum d_i^3$, where d_i – Au particle diameter; N – total number of particles observed, σ – standard deviation.
[b] from ref. [24].

Table 2
$Au 4f_{7/2}$ binding energies, Au/Al, O/Al, La/Al atomic ratios ($Au/La-Al_2O_3$) and O/(Ce+Zr), Ce/Zr, Au/Ce, Au/Zr atomic ratios ($Au/CeZrO_x$).

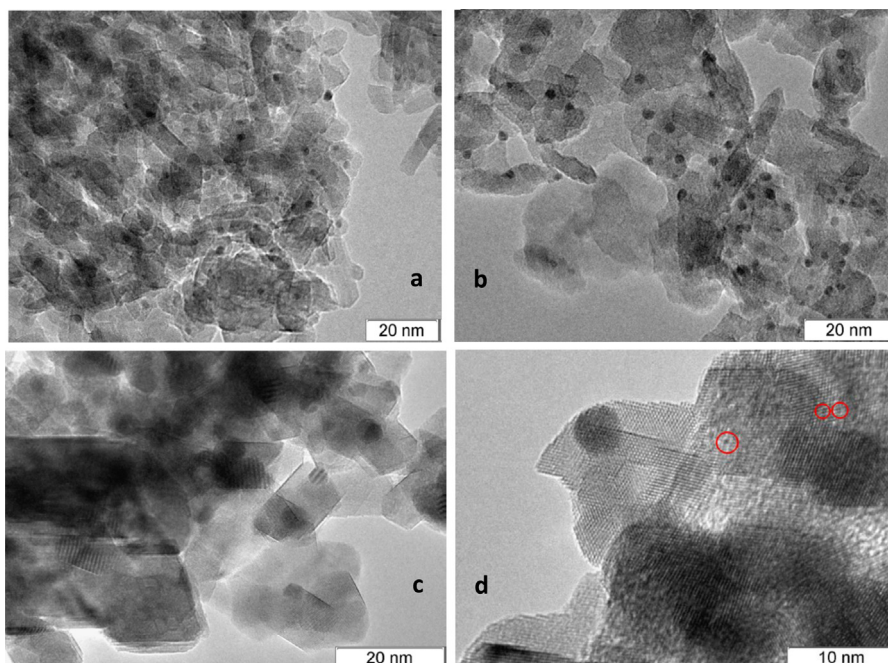| Catalyst Au/…	E_b ($Au 4f_{7/2}$) (eV)[a]	Atomic ratios[b]					
		$\frac{Au}{Al}$	$\frac{La}{Al}$	$\frac{O}{Al}$	$\frac{Au}{(Ce+Zr)}$	$\frac{Ce}{Zr}$	$\frac{O}{(Ce+Zr)}$
…La-Al_2O_3	83.8	0.005	0.013	1.41	–	–	–
…$CeZrO_x$	83.9	–	–	–	0.026	0.73	1.94

derived from the TEM study are reported in Table 1 and Fig. S1 (Supporting information), respectively. On both Al_2O_3 and La-Al_2O_3, the average Au particle sizes were clearly below 2 nm. The particle size distributions were rather narrow (Fig. S1a, b). Au particles on $CeZrO_x$ were somewhat bigger, with a broader size distribution (Figs. 1c and S1c). However, on this support, very small Au clusters, which might consist of only a few atoms, could be detected along with Au nanoparticles (Fig. 1d) as reported recently for Au/TiO_2 catalysts prepared via the same route [32,33].

X-ray photoelectron spectra of catalysts made with La-Al_2O_3 and $CeZrO_x$ supports are depicted in Fig. S2. Relevant data from these spectra are given in Table 2. From the Au $4f_{7/2}$ binding energies, gold is exclusively in the zero oxidation state. Shifts to values below the binding energy of massive gold (84.0 eV), which have been frequently reported for Au/TiO_2 catalysts (cf. discussions in ref. [34,35]), were not observed with the present supports. The lines are broader with gold on the (La-)Al_2O_3 support. Such effect is well known for materials of low conductivity where neutralization of the surface charge by the flood gun depends on a number of
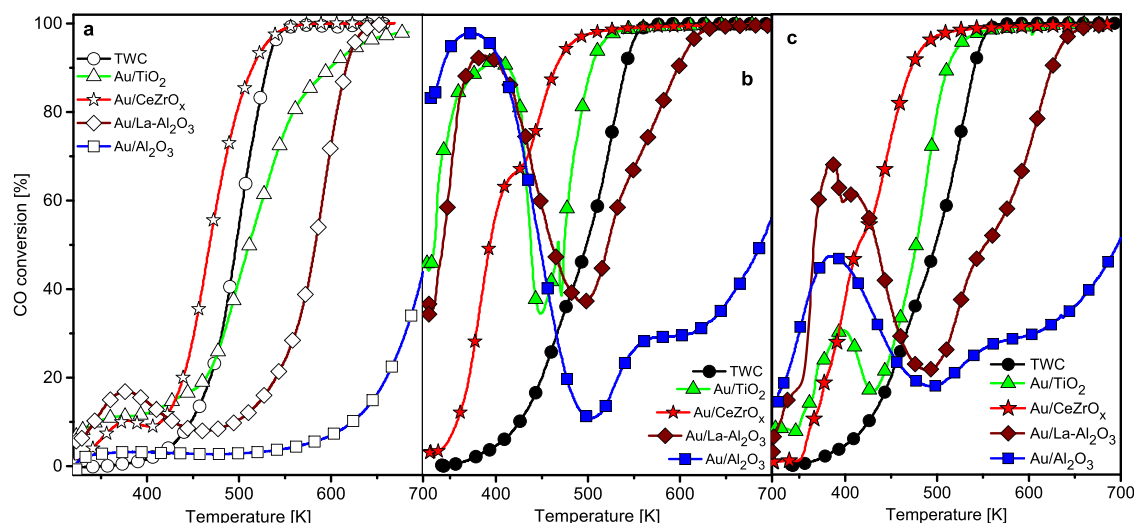
ill-defined factors (differential charging [36,37]). There are no features that could indicate the presence of Au cations in significant extent. As to the intensity data (Table 2), ratios between support cations and oxygen anions are as expected. For $Au/La-Al_2O_3$, the bulk Au/Al ratio is ≈0.005 (La neglected due to low concentration), which was just the ratio detected by XPS, i.e. there seems to be no surface enrichment in Au. However, the BET surface area plays a significant role for this discussion, and for this kind of support, the exposed support surface per Au crystallite is large. For $Au/CeZrO_x$, an Au/(Ce + Zr) ratio of 0.012 was expected while twice this value was obtained although the particles are bigger (Fig. 1). This may be understood from the significantly lower BET surface area of the support.

3.2. Reaction studies: three-way catalysis

CO, propene, and NO conversions achieved on our catalysts and the reference TWC in stoichiometric feed are summarized in

Fig. 1. TEM images of Au nanoparticles supported on Al_2O_3 (a), La-Al_2O_3 (b), and $CeZrO_x$ (c, d). For size distributions see Table 1. In d), oligomeric $(Au^0)_n$ clusters are encircled.

Fig. 2. CO conversions in stoichiometric TWC model feed as a function of catalyst temperature without water (a, empty symbols) and with 10% water (b, c, full symbols, first and second run, respectively) over Au/Al_2O_3 (blue, □,■), $Au/La-Al_2O_3$ (brown, ◇,◆), Au/TiO_2 (green, △,▲), $Au/CeZrO_x$ (red, ☆,★), and over the TWC reference catalyst (black, ○,●). For light-off temperatures see Table 2. (For interpretation of the references to colour in this figure legend, the reader is referred to the web version of this article.)

Figs. 2–4 and in Table 3. N_2O concentrations released are displayed in the inset of Fig. 4. Data for lean and rich feed are compared with those for stoichiometric feed in Figs. S3-S7.

Figs. 2 and 3 show a drastic influence of the support on the oxidation reactions, in particular on the conversion of CO in the mixture. In dry feed, it remained extremely low over Au/Al_2O_3 up to 600 K, and the light-off temperature T_{50} was well beyond 700 K (Fig. 2a). Full conversion could be observed only in an extended temperature window (up to 800 K, cf. Fig. S4 and Table 3). Notably, the propene conversion curve over Au/Al_2O_3 (Fig. 3a) was very similar to that of CO, resulting in the same light-off temperature and similar temperature of full conversion (T_{95}, cf. Table 3). The CO light-off temperature was strongly decreased already by modification of Al_2O_3 with La. It became even lower over TiO_2-supported Au, but the best CO oxidation behavior was found with Au on $CeZrO_x$, which outperformed even the reference TWC in this respect (Fig. 2a, Table 3). In propene conversion, the ranking was similar but not identical because there were different temperature lags between reaction of CO and propene: while the curves were close with $La-Al_2O_3$ ($\Delta T_{50} \approx 40$ K), CO was converted at much lower temperatures than propene over Au/TiO_2 ($\Delta T_{50} \approx 120$ K). With $Au/CeZrO_x$, the difference was smaller again (85 K), and here propene conversion occurred already in the same temperature range as over the reference TWC (Fig. 3a, Table 3).

NO reduction was dissatisfying over all monometallic Au catalysts, with conversions never exceeding 40% (Figs. 4a, S4-S7). The

unavailability of O from most NO explains why there was never full propene conversion over the Au-based catalysts. The reference TWC released considerable quantities of N_2O (up to 230 ppm, see inset in Fig. 4a). N_2O formation was lower over supported gold, which is certainly due to its lower activity for NO conversion. Over $Au/CeZrO_x$, release of 85 ppm N_2O at 30% NO conversion indicates less than 50% selectivity for N_2. At the higher temperatures of NO conversion over $Au/La-Al_2O_3$ and Au/Al_2O_3 (cf. Figs. 4a, S4b, 5b), selectivity towards N_2 was higher.

The influence of the initial oxygen content on conversions in dry feed can be observed in Figs. S3-S7. Over the reference TWC, CO was always converted at somewhat lower temperatures than propene. Full conversion was always achieved for the latter (Fig. S3d) while CO was incompletely converted in rich feed (Fig. S3c). NO conversions were indistinguishable up to ≈ 540 K ($\rightarrow 80\%$) but decreased beyond in lean feed. Under these conditions, the temperature range of N_2O formation extended far beyond the light-off region (Fig. S3b). Over the monometallic Au catalysts, there was a strong preference of CO oxidation as well, which was hardly influenced by the variations of the O_2 content. Hydrocarbon (propene) conversion was more affected by the initial O_2 content, in particular over $Au/CeZrO_x$ (Fig. S7) while the effects on NO conversion remained marginal. As a result, full NO conversion as reported in [18] was never achieved even in rich feed. Selectivity to N_2 was very sensitive to the oxygen content: N_2O formation significantly

Table 3
Light-off and full conversion temperatures in stoichiometric feed, Au catalysts compared with reference TWC.

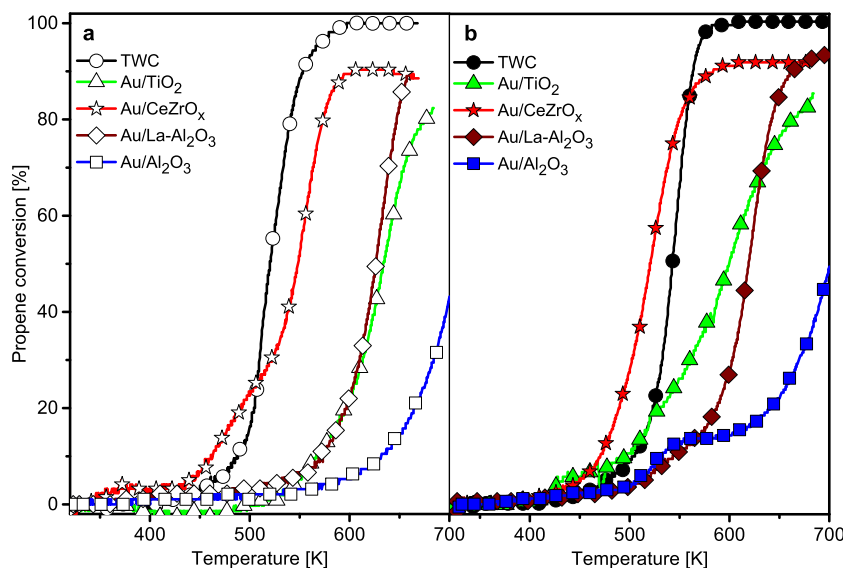| Catalyst	Light-off temperature (T_{50}), K[a]						Full conversion (T_{95}), K[b]					
	CO		Propene		NO		CO		Propene		NO	
	Dry	wet[c,d]	dry	wet[c,d]	dry	wet[c,d]	dry	wet[c,d]	dry	wet[c,d]	dry	wet[c,d]
Au/Al_2O_3	706	<300(696)	706	700(711)	–	–	771	352(>770)	755	759(766)	–	–
$Au/La-Al_2O_3$	583	341 (365)	625	618(632)	–	–	623	610 (636)	–	–	–	–
Au/TiO_2	510	332 (477)	633	600(613)	–	–	628	514 (524)	–	–	–	–
$Au/CeZrO_x$	468	392 (414)	549	520(528)	–	–	529	468 (485)	–	–	–	–
Ref. TWC	497	498 (497)	520	542	510	540	536	547 (547)	565	575	552	577

[a] Temperature of 50% conversion of the reactant.
[b] Temperature of 95% conversion.
[c] 1st run with 10 vol.-% water.
[d] 2nd run with 10 vol.-% water in parentheses.

Fig. 3. Propene conversions in stoichiometric TWC model feed as a function of catalyst temperature without water (a, empty symbols) and with 10% water (b, full symbols) over Au/Al$_2$O$_3$ (blue, □,■), Au/La-Al$_2$O$_3$ (brown, ◇,◆), Au/TiO$_2$ (green, △,▲), Au/CeZrO$_x$ (red, ☆,★), and over the TWC reference catalyst (black, ○,●). For light-off temperatures see Table 2. (For interpretation of the references to colour in this figure legend, the reader is referred to the web version of this article.)
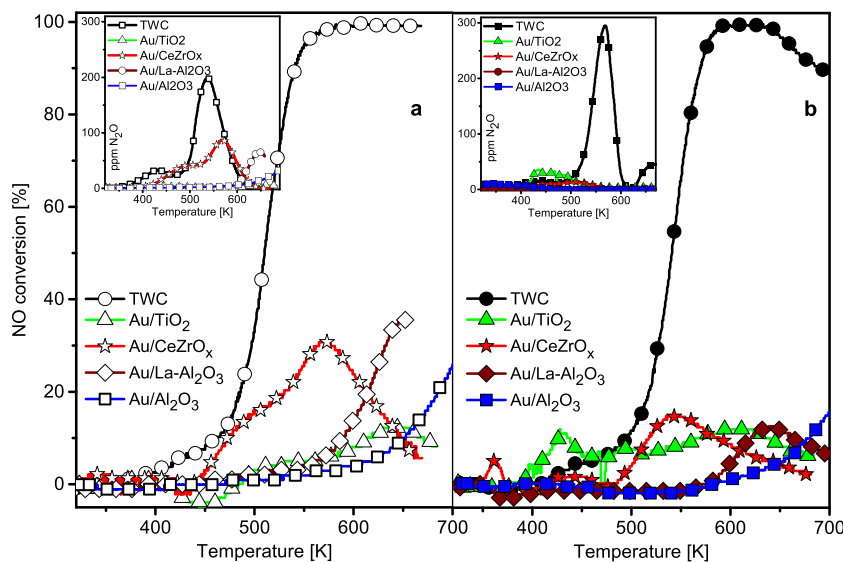
increased from rich to lean feed at hardly changed NO conversions (insets in Figs. S4b–S7b).

Light-off temperatures in moist feed (Table 3) suggest that CO conversion over the reference TWC was unaffected while conversion of propene and NO was delayed by 20–30 K (Table 3). Fig. 2 shows, however, that CO conversion was not unaffected either: it started at lower temperatures but increased with a smaller slope at growing temperature (Fig. 2a,b). N$_2$O was not suppressed by the water (Fig. 4, insets): it was now released in a single temperature range where its concentration went as high as 300 ppm.
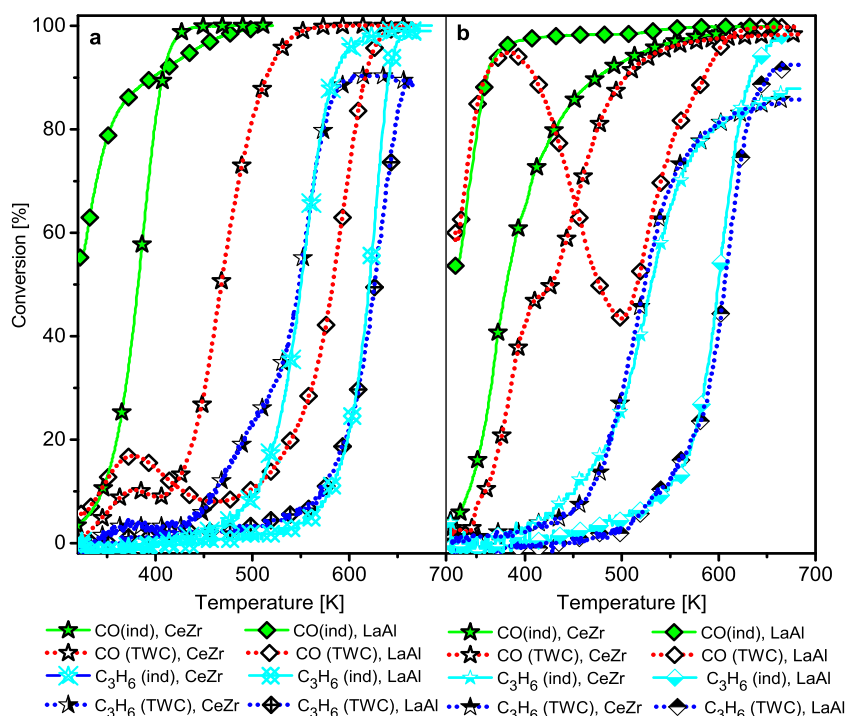
The influence of moisture on the supported Au catalysts was very pronounced. Both CO and propene were converted at lower temperatures over all catalysts (Figs. 2–4, Table 3), but while the improvement of propene conversion was marginal over some of them (Al$_2$O$_3$ and La-Al$_2$O$_3$ supports), CO conversion in the first run started at very low temperatures over all catalysts (Fig. 2b). Already

at 350–400 K, CO was almost fully converted over most of them (except for CeZrO$_x$). In these cases, conversion dropped drastically upon further temperature increase before it returned to 100% at temperatures, which were still below those required for full conversion in dry feed (Fig. 2a). It should be noted that the height of this low-temperature conversion peak was not stable: in repetitive runs it stabilized on a lower level. Fig. 2c presents data of the second run (which changed only marginally in further repeats). Over the CeZrO$_x$ support this initial conversion peak was not observed. Instead, there was a low-temperature shoulder which decreased and disappeared upon stabilization.

The different responses of the TWC and the Au-based samples to water had also some consequences for the ranking of the catalysts with respect to the oxidation reactions. As to CO oxidation, the ranking between supports remains unchanged when the low-temperature conversion peaks are disregarded. The reference

Fig. 4. NO conversions and N$_2$O concentrations (insets) in stoichiometric TWC model feed as a function of catalyst temperature without water (a, empty symbols) and with 10% water (b, full symbols) over Au/Al$_2$O$_3$ (blue, □,■), Au/La-Al$_2$O$_3$ (brown, ◇,◆), Au/TiO$_2$ (green, △,▲), Au/CeZrO$_x$ (red, ☆,★), and over the TWC reference catalyst (black, ○,●). For light-off temperatures see Table 2. (For interpretation of the references to colour in this figure legend, the reader is referred to the web version of this article.)

Fig. 5. CO and propene conversions in stoichiometric feeds comprising CO (or propene) and oxygen only ("ind": 1.1% CO, 0.55% O_2, or 0.1% propene, 0.45% O_2) or the complete TWC model feed, a − dry feed, b − moist feed, 10% H_2O.

TWC was outperformed even by Au/TiO$_2$ in presence of moisture (Fig. 2b). While the performance of Au/TiO$_2$ and Au/La-Al$_2$O$_3$ in propene oxidation was quite similar in dry feed, the former became superior in the presence of water due to its stronger susceptibility to the moisture effect (Fig. 3a,b). Likewise, Au/CeZrO$_x$ outperformed the reference TWC in moist feed even with respect to light-off of propene conversion, which did not, however, become complete due to unavailability of the NO oxidant over the gold catalyst (Fig. 3b).

The effect of moisture on NO reduction was negative in all cases, with the exception of some low-temperature conversion over Au/TiO$_2$ (Fig. 4). N$_2$O formation was, however, strongly suppressed (Fig. 4, insets), again with the exception of low-temperature NO conversion over Au/TiO$_2$, where N$_2$O selectivity was estimated to be >50%. Where NO conversion peaks occurred above 500 K, N$_2$ selectivity was ≥90%, growing with increasing temperature.

3.3. Reaction studies: oxidation of CO and of propene, NO reduction by CO
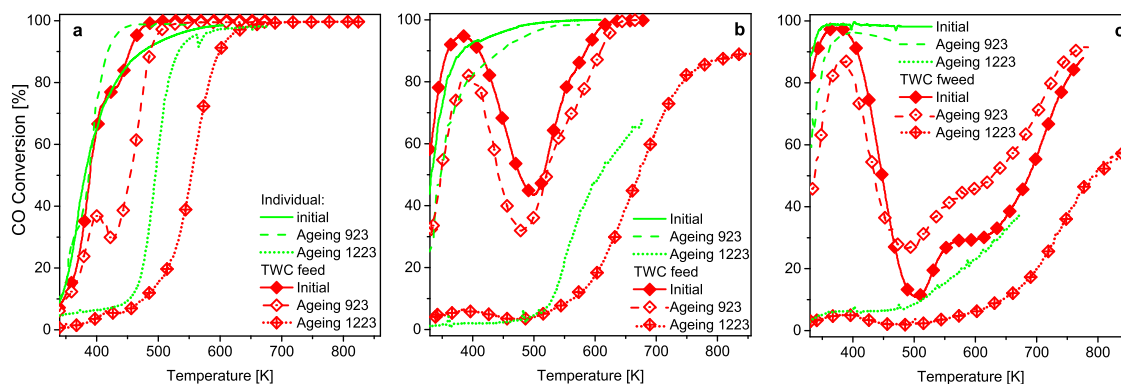
Results of CO and propene oxidation on Au/La-Al$_2$O$_3$ and on Au/CeZrO$_x$ are summarized in Fig. 5 where conversions of CO and propene fed individually to a stoichiometric O$_2$ amount are compared with conversions in the stoichiometric TWC model mixture in dry feed (a) and in moist feed (b). Data for the TWC feed originate from repeated measurements (first run with fresh catalysts, remaining experiments subsequently with the same sample), which resulted in some deviations from results shown in Fig. 2. These were always negligible in dry feed while some light-off temperatures were increased by 15–35 K in moist feed for unknown reasons.

The influence of co-reactants was dramatic in CO conversion, but negligible in propene conversion. CO oxidation over La-Al$_2$O$_3$ is a particular drastic case. Its light-off temperature in dry CO/O$_2$ feed (Fig. 5a) was below 320 K and full conversion was reached at 440 K as would have been expected for a gold catalyst. In TWC feed, a minor conversion peak occurred at 375 K, with a peak conversion

just about 20%. Upon temperature increase, the CO oxidation rate decreased again and went off only well above 500 K, with T$_{50}$ of 583 K and full conversion around 623 K. CeZrO$_x$-supported gold was less active than Au/La-Al$_2$O$_3$ in oxidation of CO alone but behaved more favourably in the TWC feed. However, an interaction between the reactants could be noted here as well: In the TWC feed, CO oxidation started in the same temperature range as in the individual feed (slightly above 300 K), but went into a plateau of ca. 10% conversion between 370 and 400 K before it started off to full conversion. In propene oxidation, the differences between conversion in O$_2$ alone and in TWC feed were marginal over both catalysts. With the CeZrO$_x$ support, propene conversion exhibited a plateau in the same temperature range as CO conversion. Both conversions began to increase at the same temperature, initially with a smaller slope for propene. Over the La-Al$_2$O$_3$ support, parallel tendencies were less pronounced.

In moist feed (Fig. 5b), CO conversions over Au/La-Al$_2$O$_3$ were identical within experimental error up to 370 K, where full conversion was achieved also in the TWC feed (1st run, cf. Fig. 2b). With growing temperature, conversion went through the minimum described earlier in TWC feed, but stayed near 100% in the whole temperature range in absence of propene and NO. Over the CeZrO$_x$ support, the influence of propene and NO was much smaller in moist feed. While the oxidation of CO alone was not significantly affected by the water, its conversion in the mixture was strongly improved. Therefore, both light-off curves are rather close, with only a slight shoulder in that of the mixed feed. Propene conversions again were not influenced by the presence of CO and NO. Notably, analogies in the profiles of CO and propene that were observed in dry feed (e.g. for Au/CeZrO$_x$) disappeared in the presence of water.

In Fig. S8, conversions of NO and CO are summarized for NO reduction, and NO conversions in the full model mixture (all without water) are added for comparison. Dramatic differences in reactivity can be seen in these data as well. Over Au/CeZrO$_x$ (Fig. S8b), NO conversions in the binary feed and in the full mixture were very close at low temperatures while they diverged at 570 K,

Fig. 6. Impact of high-temperature treatments (5% O_2, 10% H_2O, 6 h at 923 K or 1223 K) on CO conversion in CO oxidation and in complete TWC model feed (with 10% H_2O in both cases), a − Au/CeZrO$_x$, b − Au/La-Al$_2$O$_3$, c − Au/γ-Al$_2$O$_3$.

further increasing in the binary feed but decreasing in the model exhaust. N_2O was released at similar rates in both experiments (Fig. S8b, inset), starting at lower temperatures in the binary feed. However, since initial NO concentration was higher in the binary feed, the N_2O selectivity was significantly less in absence of propene and oxygen. On the La-Al$_2$O$_3$ support, Au is able to reduce NO by CO already at very low temperatures (Fig. S8a) though again with significant selectivity to N_2O, in particular below 400 K. Both conversions reached a plateau around 470 K and did not increase any more below 600 K. At the same time N_2O selectivity decreased strongly with growing temperature, and selectivity to nitrogen became complete above 520 K. Opposed to this, NO conversion started only around 520 K in the full mixture reaching a peak around 650 K. Only in this temperature range, N_2O formation was observed in significant quantities.

3.4. Thermal stability

The impact of high-temperature treatments (6 h, 5% O_2, 10% H_2O) on the catalytic behavior of supported Au catalysts is summarized in Figs. 6 and 7. At the present stage, we are communicating reactivity data only, while we are now studying structural changes behind these effects.

In Fig. 6, CO conversions in binary feed and in the full TWC feed are compared. On all supports studied, calcination at 923 K had only a moderate influence on CO conversion both in the binary and in the TWC feed. Over Au/CeZrO$_x$ (Fig. 6a), full conversion in the binary feed was achieved even at lower temperature after the treatment. In the TWC mixture, CO conversion started almost at the same temperatures after calcination as in the initial state. However, the characteristic shoulder at the conversion curve of the initial sample (at ≈60% conversion in Fig. 1b, at ≈80% conversion in Fig. 6a), which is reminiscent of the pronounced conversion peaks on the non-reducible supports, was converted into a minor conversion peak by the thermal stress. As a result, the light-off temperature increased by ≈60 K. On the Al$_2$O$_3$-based supports, the impact of the calcination on CO conversion is somewhat different (Fig. 6b,c). In both cases the conversion curve was shifted to higher temperatures by ca. 20 K already in the binary feed. Correspondingly the increase of low-temperature CO conversion was somewhat delayed also in the full mixture, and as the poisoning influence appears to become effective at the same temperature as with the initial sample, the CO conversion peaks became lower with these supports. On La-Al$_2$O$_3$ (Fig. 6b), the recovery of CO conversion was slightly shifted to higher temperatures likewise. Notably, over calcined Au/Al$_2$O$_3$ this rise happened at significantly lower temperatures. This is a reproducible result: the same observation was made with gold (2 wt-%) on δ-Al$_2$O$_3$, which was subjected to a redox cycling treatment as

described in [38,39] ({2% CO/He, 15 min → 2% O_2/He, 15 min}, 5 repeats at 923 K) [40].
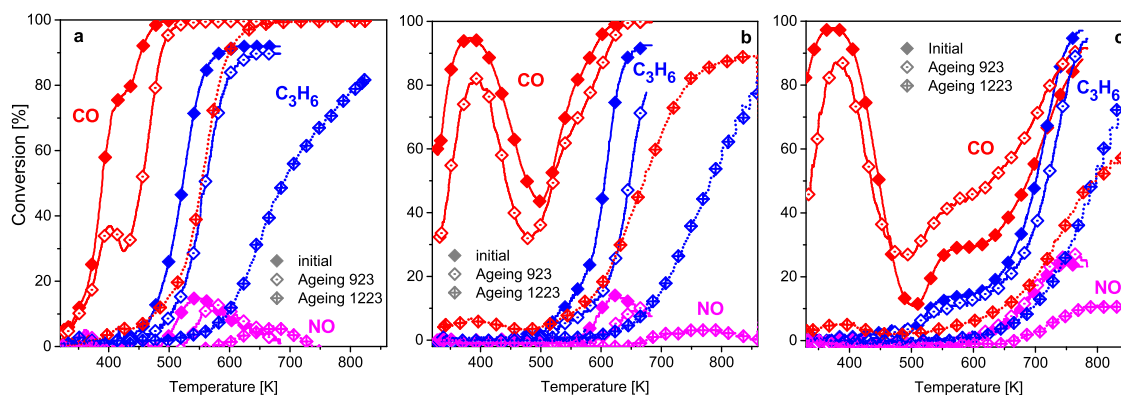
Ageing at 1223 K deteriorated the properties of gold on all supports investigated. However, the effect was surprisingly moderate on CeZrO$_x$. In the binary feed, the light-off happened at respectable 497 K while 553 K were required to convert 50% of CO in the model feed where shoulders or peaks resulting from sites operating at low temperatures were completely removed (Fig. 6a). The same happened on the non-reducible supports (Fig. 6b,c), but as the low-temperature performance is more spectacular there, deactivation appears more dramatic. However, even the second rise of conversion was more delayed on these supports: the upshift of the respective light-off temperatures between calcinations at 923 K and 1223 K is 100 K for Au/CeZrO$_x$, 150 K for Au/La-Al$_2$O$_3$, and 170 K for Au/Al$_2$O$_3$.

In Fig. 7, the effect of thermal treatments on the conversion of the remaining feed components is shown. Calcination at 923 K caused only moderate changes in propene conversion as well, in particular with Au/γ-Al$_2$O$_3$ (Fig. 7c) where, however, activity was low anyway. The impact of calcination at 1223 K was much more severe. Although the damage appears to be less pronounced with the alumina support (Fig. 7c), this catalyst remained the least active one (T_{50} = 800 K) shortly after Au/La-Al$_2$O$_3$ (T_{50} = 783 K) while the residual activity of Au/CeZrO$_x$ was considerably higher (T_{50} = 688 K).

4. Discussion

The results of the catalytic experiments reveal strong competition between reactants for Au oxidation sites and significant influences of the support and of feed moisture on this competition. On some supports, these interactions delayed CO oxidation drastically in dry feed, but the poisoning was attenuated in presence of water (Fig. 2). This improved the performance of gold in oxidation reactions on all supports, on some of them beyond the performance of a reference TWC (Figs. 2 and 3). Au is also able to catalyze NO reduction, but the rates are too low to allow anticipating a positive contribution in a fully formulated TWC. Full NO conversion as reported in ref. [18] for Au on a multi-oxide support (both in presence of some Rh, but also without a second noble metal) was not observed with any of the supports tested in our study (Fig. 4). Where NO was reduced at low temperatures, selectivity to N_2O was high, but it became lower when NO reduction occurred at higher temperatures, and was further suppressed by moisture. This differs from the behavior of the noble metals in the reference TWC (Fig. 4).

In dry feed, there is a clear ranking of CO oxidation activity, which reminds the differentiation of Au-support interactions in terms of support reducibility ("inactive – active" supports [41]). Au seems to be most active on CeZrO$_x$, less active on TiO$_2$, and most

Fig. 7. Impact of high-temperature treatments (5% O_2, 10% H_2O, 6 h at 923 K or 1223 K) on propene and NO conversion in complete TWC model feed (incl. 10% H_2O in both cases), CO conversion added for comparison; a − Au/CeZrO$_x$, b − Au/La-Al$_2$O$_3$, c − Au/γ-Al$_2$O$_3$.

inactive on Al$_2$O$_3$ (Fig. 2a). In this comparison, the effect of La is interesting, given its low surface concentration ((La/Al)$_{XPS}$ = 0.013, Table 2). Although the La/Al ratio might be higher at the external surface due to averaging nature and finite sampling depth of XPS, it is obvious that the support still exposes way more Al than La cations. The significant effect of La on CO conversion in dry TWC feed (Fig. 2a) and on other properties as well (see below) may therefore indicate that Au prefers to interact with La-containing patches of the Al$_2$O$_3$ surface.

Comparison of these data with results of CO and propene oxidation in absence of co-reactants shows that it is actually the competition with other components for sites which is modified by the support. In absence of NO and propene, Au is even more active on La-Al$_2$O$_3$ than on CeZrO$_x$ (Fig. 5a), in obvious contradiction to the "(in)"active support rationale. The reason for this is unclear. From the Au particle sizes (Table 1), the exposed Au surface area on CeZrO$_x$ may have been ca. 50% that of La-Al$_2$O$_3$, but the difference in activity is an order of magnitude rather than 50%. Supported monoatomic or oligomeric (Au^0)$_n$ clusters have recently been considered as sites of particular high CO oxidation activity [32,42,43], but although such sites were apparently detected on Au/CeZrO$_x$ by TEM (Fig. 1d) this did not alleviate the difference in catalytic behavior.

To solve the question if CO oxidation is poisoned by propene or by NO, we performed the relevant reactions (CO or propene oxidation, NO reduction by CO) individually. In Fig. 5, it can be seen that propene oxidation is not influenced to any significant extent by the presence of CO or NO. On the contrary, the poisoning effect is very visible in CO oxidation, and it is much stronger with the non-reducible La-Al$_2$O$_3$ than with the reducible CeZrO$_x$ support. In NO reduction by CO (Fig. S8), a similar picture can be observed: the reaction proceeded already at low temperatures over Au/La-Al$_2$O$_3$, but was quenched in the full TWC mixture (Fig. S8a). Over Au/CeZrO$_x$, the quenching effect was small, even negligible: NO conversions in binary feed and in the full mixture started to increase in the same temperature range. From the similar ranking of poisoning efficiencies in CO oxidation and NO reduction over the two supports we conclude that the component missing in these reactions, i.e. propene, is the poison.

The identification of propene as a poison for CO and NO oxidation suggests some ideas that might explain the relation between support reducibility and intensity of the poisoning effect. CO oxidation over Au on reducible supports as Fe$_2$O$_3$, TiO$_2$ and Ce-containing oxides is usually ascribed to Au sites at the perimeter between Au and the support that cooperate with adjacent support sites [11,32,44]. The interaction with the gold tends to activate adjacent sections of the support surface which contribute more active oxygen than the bare support would do [45]. Poisoning by hydrocarbons most likely occurs by deposition of incompletely oxidized species on the perimeter sites. When more active oxygen is available (e.g. on CeZrO$_x$) these species can be removed by complete oxidation at lower temperatures. Although reducibility of La$_2$O$_3$ is certainly low, the poisoning effect of propene on the Au sites was clearly weaker on La-Al$_2$O$_3$ than on Al$_2$O$_3$ (Fig. 2). This confirms that Au particles had La-modified surface sections in their vicinity.

Feed water apparently competes strongly with propene adsorption, but leaves CO adsorption unaffected: on the La-Al$_2$O$_3$ support, CO oxidation was identical in the reaction of TWC feed and of CO alone at low temperatures (Fig. 5b). Only above 380 K, propene appears to interact, and interaction efficiency increasing with temperature suggests that we deal with an activated chemisorption. In dry feed the poisoning is significant already at 320 K, but here as well, a temperature region with decreasing CO conversion can be observed (Fig. 5a). The ultimate rise of CO conversions happens at higher temperatures than in moist feed, which also supports the attenuation of propene poisoning by water. On the CeZrO$_x$ support, the less pronounced influence of propene on CO oxidation is further suppressed in presence of water, which resulted in a rather weak effect (Fig. 5b).

The decay of the low-temperature CO conversion peak in the repetitive runs (Fig. 2b,c) seems to indicate a low stability of the gold catalysts. However, other results suggest that the change may be related to incomplete removal of residues rather to than to structural changes. Deactivation affects mainly the low-temperature features. In dry feed where those are missing, loss of activity was much less pronounced or even absent. Much smaller losses of low-temperature performance were observed with Au/La-Al$_2$O$_3$ and Au/Al$_2$O$_3$ after calcination in moist dilute air at even 923 K (Fig. 7b,c). Therefore, a thermal effect is unlikely to be the reason for deactivation after a run up to just 700 K (Fig. 2b,c). Moreover, the series of experiments in Fig. 5 were started with a run in full TWC feed followed by the runs of CO and propene oxidation. Therefore, the spectacular conversion curve of CO oxidation in CO/O$_2$ over Au/La-Al$_2$O$_3$ (Fig. 5b) was recorded with a catalyst surface which would have produced the CO conversion curve depicted in Fig. 2c if the full TWC mixture had been fed instead of CO/O$_2$. This shows clearly that CO oxidation is not the problem, rather, the interaction of propene with the catalyst becomes more intense in the second run. Deposits left after the first run offering a stronger interaction to propene than the bare alumina surface, may be a reason for this. Future research will deal with the nature of these deposits, how they can be avoided or removed by regeneration.

The durability tests (Figs. 6 and 7) show that monometallic supported Au catalysts could well be used at temperatures up to 923 K. The excellent stability of Au catalysts has been described already earlier in particular for alumina supports [21–23], but we find here

that stability is even superior with Au/CeZrO$_x$. CO oxidation in binary feed over this catalyst is almost not affected by the treatment (Fig. 6a), and the nearly identical onset of the corresponding CO conversion curves shows that this holds also for the full mixture. The following minor peak in the curve after thermal stress, which results in the 60 K upshift of the light-off temperature, may result from a structural stabilization of the support surface, which would provide less active oxygen after the treatment than in the initial state. Propene oxidation and NO reduction are somewhat stronger affected by the calcination (Fig. 7a).

While all three reactions are suppressed to a rather similar extent by the treatment on Au/La-Al$_2$O$_3$ (Figs. 6b and 7b), Au/Al$_2$O$_3$ offers some surprises: its activity for CO oxidation suffers to a similar extent as with Au/La-Al$_2$O$_3$, but the recovery of CO conversion from the poisoning effect occurs at lower temperatures after calcination (Fig. 6c). The reason for this effect is unclear. Propene oxidation and NO reduction remain almost unaffected by the thermal stress over this catalyst, however, on a low activity level (Fig. 7c). After thermal treatment at 1223 K, all conversion curves are significantly shifted to higher temperatures. Still, there is remarkable residual oxidation activity towards CO and even propene, but light-off temperatures are too high for practical purposes.

In summary, the potential of supported gold for TWC applications is compromised by a strong interaction of the hydrocarbon component (propene) with the active sites, which poisons CO conversion at low temperatures, and by the low NO reduction activity of gold. The poisoning effect is alleviated by reducible supports (CeZrO$_x$), and is less severe in the presence of water. Therefore, Au/CeZrO$_x$ competes favorably with a Pd-based commercial three-way catalyst in the oxidation reactions. However, as expected, monometallic Au catalysts do not cope with the thermal stability requirements related to TWC applications. Therefore, opportunities for Au in three-way catalysis should be sought in alloys with an element that might contribute both NO reduction activity and thermal stability, e.g. Pd.

5. Conclusions

In the reaction of stoichiometric model mixtures for gasoline car exhaust (comprising CO, propene, NO, O$_2$, with or without water) over supported monometallic Au catalysts, propene was observed to exert strong poisoning effects on CO oxidation. The poisoning effect depended on the nature of the support and on the water content of the gas being most intense in dry feed but partly alleviated in presence of moisture. The effect was most pronounced with Au on Al$_2$O$_3$, but its intensity decreased when La-Al$_2$O$_3$ and TiO$_2$ supports were employed, und was rather weak with CeZrO$_2$. While Au exhibited promising catalytic potential for oxidation of CO and propene in particular when supported on CeZrO$_x$, NO was only partly converted. When this conversion occurred at low temperatures, selectivity to N$_2$O was significant while N$_2$ was predominantly formed at higher temperatures. Supported Au catalysts were only moderately deactivated by calcination in moist dilute air at 923 K. The best durability was found for Au on a CeZrO$_x$ support where CO oxidation in binary feed (equimolar CO/O$_2$) was not significantly affected at all while the poisoning effect of propene became more severe in the TWC model feed. Analogous treatment at 1223 K resulted in inacceptable damage to all reactions involved and on all supports.

Appendix A. Supplementary data

Supplementary data associated with this article can be found, in the online version, at http://dx.doi.org/10.1016/j.apcatb.2016.10.017.

References

[1] M. Haruta, T. Kobayashi, H. Sano, N. Yamada, Chem. Lett. (1987) 405–408.
[2] M. Haruta, Cattech 6 (2004) 102–115.
[3] B. Schumacher, V. Plzak, J. Cai, R.J. Behm, Catal. Lett. 101 (2005) 215–224.
[4] S. Minico, S. Scire, C. Crisafulli, S. Galvagno, Appl. Catal. B 34 (2001) 277–285.
[5] W.L. Deng, J. De Jesus, H. Saltsburg, M. Flytzani-Stephanopoulos, Appl. Catal. A 291 (2005) 126–135.
[6] K. Ruth, M. Hayes, R. Burch, S. Tsubota, M. Haruta, Appl. Catal. B 24 (2000) L133–L138.
[7] C. Cellier, S. Lambert, E.M. Gaigneaux, C. Poleunis, V. Ruaux, P. Eloy, C. Lahousse, P. Bertrand, J.P. Pirard, P. Grange, Appl. Catal. B 70 (2007) 406–416.
[8] T. Hayashi, K. Tanaka, M. Haruta, J. Catal. 178 (1998) 566.
[9] P. Landon, P.J. Collier, A.J. Papworth, C.J. Kiely, G.J. Hutchings, Chem. Commun. (2002) 2058–2059.
[10] B. Nkosi, N.J. Coville, G.J. Hutchings, Appl. Catal. 43 (1988) 33–39.
[11] G.C. Bond, C. Louis, D.T. Thompson, Catalyis by Gold, Imperial College Press, London, 2006.
[12] C. Bianchi, F. Porta, L. Prati, M. Rossi, Top. Catal. 13 (2000) 231–236.
[13] L. Prati, A. Villa, C.E. Chan-Thaw, R. Arrigo, D. Wang, D.S. Su, Faraday Discuss. 152 (2011) 353–365.
[14] A. Ueda, M. Haruta, Gold Bull. 32 (1999) 3–11.
[15] L.Q. Nguyen, C. Salim, H. Hinode, Appl. Catal. A 347 (2008) 94–99.
[16] X.K. Wang, A.Q. Wang, X.D. Wang, T. Zhang, X.F. Yang, React. Kinet. Cataly. Lett. 92 (2007) 33–39.
[17] E. Seker, E. Gulari, Appl. Catal. A 232 (2002) 203–217.
[18] J.R. Mellor, A.N. Palazov, B.S. Grigorova, J.F. Greyling, K. Reddy, M.P. Letsoalo, J.H. Marsh, Catal. Today 72 (2002) 145–156.
[19] I.L. Simakova, Y.S. Solkina, B.L. Moroz, O.A. Simakova, S.I. Reshetnikov, I.P. Prosvi-rin, V.I. Bukhtiyarov, V.N. Parmon, D.Y. Murzin, Appl. Catal. A 385 (2010) 136–143.
[20] Z. Ma, S. Dai, Heterogeneous gold catalysts and catalysis, R. Soc. Chem. (2014) 1–26.
[21] G.N. Ilinich, B.L. Moroz, N.A. Rudina, I.P. Prosvirin, V.I. Bukhtiyarov, Carbon 50 (2012) 1186–1196.
[22] B.L. Moroz, D.A. Zuizin, V.I. Zaikovskii, A.N. Shmakov, P.A. Pyryaev, E.M. Moroz, V.I. Bukhtiyarov, HRTEM and PDF evidences for epitaxial gold-support interaction in the nanodispersed Au/Al$_2$O$_3$ catalysts for low-temperature CO oxidation, Europacat IX, Salamanca (2009) 10–108.
[23] I.L. Simakova, Y.S. Solkina, B.L. Moroz, S.I. Reshetnikov, I.P. Prosvirin, V.I. Bukhti-yarov, D.Y. Murzin, Appl. Catal. A 385 (2010) 136–143.
[24] Strem Chemicals, Technical note for Au/TiO$_2$, https://secure.strem.com/catalog/v/79-0165/25/gold_7440-57-5, accessed October 13, 2016.
[25] S. Tsubota, M. Haruta, T. Kobayashi, A. Ueda, Y. Nakahara, Stud. Surf. Sci. Catal. 63 (1991) 695–704.
[26] B.L. Moroz, P.A. Pyrjaev, V.I. Zaikovskii, V.I. Bukhtiyarov, Catal. Today 144 (2009) 292–305.
[27] J.R. Anderson, Structure of Metallic Catalysts, Academic Press, London, 1975.
[28] J.H. Scofield, J. Electron Spectrosc. Relat. Phenom. 8 (1976) 129–137.
[29] M.P. Gonzalez-Marcos, B. Pereda-Ayo, A. Aranzabal, J.A. Gonzalez-Marcos, J.R. Gonzalez-Velasco, Catal. Today 180 (2012) 88–95.
[30] S.B. Kang, S.J. Han, S.B. Nam, I.-S. Nam, B.K. Cho, C.H. Kim, S.H. Oh, Chem. Eng. J. 207–208 (2012) 117–121.
[31] E.J. Lox, in: G. Ertl, H. Knözinger, F. Schüth, J. Weitkamp (Eds.), Handbook of Heterogeneous Catalysis, 2 ed., Wiley-VCH, Weinheim, 2008, p. 2274.
[32] W. Grünert, D. Großmann, H. Noei, M.M. Pohl, I. Sinev, A. De Toni, Y. Wang, M. Muhler, Angew. Chem. Int. Ed. 53 (2014) 3245–3249.
[33] W. Grünert, D. Grossmann, H. Noei, M.M. Pohl, I. Sinev, A. De Toni, Y.M. Wang, M. Muhler, Chemie Ing. Techn. 86 (2014) 1883–1889.
[34] W. Grünert, A. Brückner, H. Hofmeister, P. Claus, J. Phys. Chem. B 108 (2004) 5709–5717.
[35] N. Kruse, S. Chenakin, Appl. Catal. A 391 (2011) 367–376.
[37] W. Grünert, in: M. Che, J.C Vedrine (Eds.), Characterisation of Solid Materials: From Structure to Surface Reactivity, Wiley-VCH, Weinheim, 2012, pp. 537–583.
[38] S. Heikens, 2014. Darstellung und Charakterisierung edelmetalldotierter La-, Fe-, Co-Perowskite als selbstregenerierende Katalysatoren in der Dreiwegekatalyse, PhD Thesis, Bochum, http://www-brs.ub.ruhr-uni-bochum.de/netahtml/HSS/Diss/HeikensSascha/.
[39] B. Saruhan, G.C. Mondragón Rodríguez, A.A. Haidry, A. Yüce, S. Heikens, W. Grünert, Adv. Eng. Mat. 18 (2016) 728–738.

[40] V. Ulrich, W. Grünert, B., Moroz, P. Pyriaev, V.I. Bukhtiyarov, unpublished results.

[41] M.M. Schubert, S. Hackenberg, A.C. van Veen, M. Muhler, V. Plzak, R.J. Behm, J. Catal. 197 (2001) 113–122.

[42] A.A. Herzing, C.J. Kiely, A.F. Carley, P. Landon, G.J. Hutchings, Science 321 (2008) 1331–1335.

[43] M.W.E. van den Berg, A. De Toni, M. Bandyopadhyay, H. Gies, W. Grünert, Appl. Catal. A 391 (2011) 268–280.

[44] M.F. Camellone, J.L. Zhao, L.Y. Jin, Y.M. Wang, M. Muhler, D. Marx, Angew. Chem. Intern. Ed. 52 (2013) 5780–5784.

[45] D. Widmann, R.J. Behm, Acc. Chem. Res. 47 (2014) 740–749.